

# Comparison of Heterogeneous and Homogenized Numerical Models of Cavitation

*Roman Samulyak*<sup>1,\*</sup> *Yarema Prykarpatsky*<sup>3</sup> *Tianshi Lu*<sup>1</sup>  
*James Glimm*<sup>1,2</sup> *Zhiliang Xu*<sup>2</sup> & *Myoung-Nyoun Kim*<sup>4</sup>

<sup>1</sup> *Computational Science Center, Brookhaven National Laboratory, Upton, NY 11973, USA*

<sup>2</sup> *Department of Applied Mathematics and Statistics, SUNY at Stony Brook, Stony Brook, NY 11794, USA*

<sup>3</sup> *WMS, AGH University of Science and Technology, Al. Mickiewicza 30, 30059 Krakow, Poland*

<sup>4</sup> *Department of Mathematics, Kyushu University, Fukuoka-city, 812-8581 Japan*

## ABSTRACT

---

*We have studied two approaches to the modeling of bubbly and cavitating fluids. The heterogeneous approach is based on the direct numerical simulation of gas bubbles using the interface tracking technique. The second one uses a homogenized description of bubbly fluid properties. Two techniques are complementary and can be applied to resolve different spatial scales in simulations. Numerical simulations of the dynamics of linear and shock waves in bubbly fluids have been performed and compared to experiments and theoretical predictions. Two techniques have been applied to the study of hydrodynamic processes in liquid mercury targets for a new generation of accelerators.*

---

\*Address all correspondence to [rosamu@bnl.gov](mailto:rosamu@bnl.gov)

## 1. INTRODUCTION

An accurate description of cavitation and wave propagation in cavitating and bubbly fluids is a key problem in modeling and simulation of hydrodynamic processes in a variety of applications ranging from marine engineering to high-energy physics. The modeling of free surface flows imposes an additional complication on this multiscale problem.

The wave propagation in bubbly fluids has been studied using a variety of methods. Significant progress has been achieved using various homogenized descriptions of multiphase systems (see, for example, [1–4] and references therein). The Rayleigh-Plesset equation for the evolution of the average bubble size distribution has often been used as a dynamic closure for fluid dynamics equations. This allows one to implicitly include many important physics effects in bubbly systems. Numerical simulations of such systems require relatively simple and computationally inexpensive numerical algorithms. To model cavitating and bubbly fluids within the homogeneous approximation, we have recently developed and implemented in FronTier, a compressible hydrodynamics code with free interface support [5], a two-phase equation of state (EOS) model based on the isentropic approximation [6]. Homogenized models can effectively be used for large systems, especially if the resolving of spatial scales smaller than the distance between bubbles is not necessary. Nevertheless, homogenized models cannot capture all features of complex flow regimes and exhibit sometimes large discrepancies with experiments [3] even for systems of nondissolvable gas bubbles.

The heterogeneous method (or direct numerical simulation) is a powerful method for multiphase problems based on techniques developed for free surface flows. The heterogeneous method is potentially a very accurate technique, limited by only numerical errors. It allows to account for drag, surface tension, and viscous forces as well as the phase transition induced mass transfer. Examples of numerical simulations of a single vapor bubble undergoing a phase transition on its surface are given in [7,8]. Systems of bubbles in fluids were modeled in [9] using the incompressible flow approximation for both fluid and vapor and a simplified version of the interface tracking. In this paper, we develop a heteroge-

neous numerical simulation method for bubbly and cavitating flows based on an explicit numerical resolution of systems of compressible bubbles in fluids using the method of front tracking. Our FronTier code is capable of tracking and resolving topological changes of a large number of fluid interfaces in two-dimensional (2D) and three-dimensional (3D) spaces. We present the simulation results of the wave dynamics of linear and shock waves in bubbly systems and compare them to classical experiments. The direct numerical simulations of bubbly fluids in large 3D domains remain, however, prohibitively expensive even on supercomputers.

Therefore, both heterogeneous and homogenized approaches have advantages and disadvantages and can be used to resolve different temporal and spatial scales in numerical simulations. In this paper, we present results of the validation and comparison of our heterogeneous and homogenized numerical simulation models and discuss their applicability range and limitations.

Two numerical approaches are being used in the study of hydrodynamic processes involving cavitation and bubble dynamics in the liquid mercury target for the Neutrino Factory/Muon Collider, a proposed future advanced accelerator [10], <http://www.cap.bnl.gov/mumu/info/intro.html>. The target has been proposed as a liquid mercury jet interacting with an intense proton pulse in a 20 Tesla magnetic field. The state of the target after the interaction with a pulse of protons depositing a large amount of energy into mercury (the peak energy deposition is about 100 J/g) is of major importance to the accelerator design. This paper deals only with hydrodynamic aspects of the problem, namely, the jet evolution after the interaction with a proton pulse and cavitation of mercury in strong rarefaction waves. MHD processes have been studied in a separate work.

The paper is organized as follows. In Section 2, we describe the homogenized EOS model for multiphase flows and the heterogeneous simulation method as well as results of the wave dynamics study in bubbly fluids using the heterogeneous method and their comparison with experiments and theoretical predictions. Section 3 presents results of the numerical simulation of the liquid mercury jet interacting with high-intensity proton pulses using two cavitation modeling techniques. We compare simulation results obtained with two methods and

discuss their applicability and limitations. We conclude the paper with a summary of our results and perspectives for future work.

## 2. MODELING OF MULTIPHASE FLOWS

### 2.1 Homogenized Model

The homogeneous flow approximation provides a simple technique for analyzing two-phase (or multiple phase) flows. It is sufficiently accurate to handle a variety of practically important processes. Suitable averaging is performed over the length scale, which is large compared to the distance between bubbles, and the mixture is treated as a pseudofluid that obeys an equation of state (EOS) of a single component flow.

We have recently developed [6] a simple isentropic homogenized equation of state for two-phase liquids and implemented the corresponding software library in *FrontTier*, a compressible hydrodynamics code with free interface support [5] based on the method of front tracking [11]. The bubbly and/or cavitating liquid is described by the system of equations of compressible hydrodynamics for a single component fluid. The equation of state, which closes this system, describes averaged physics properties of the bubbly liquid at given values of the void fraction. The isentropic approximation reduces by one the number on independent variables defining the thermodynamic state. As a result, all thermodynamic states in our EOS are functions of only density.

The proposed EOS consists of three branches. The pure vapor branch is described by the polytropic EOS

$$P = (\gamma_v - 1)E\rho \quad (1)$$

where  $P$  is the pressure,  $\rho$  is the density,  $E$  is the specific internal energy, and  $\gamma_v$  is the adiabatic exponent for the vapor. Reducing this expression to an isentrope, we obtain

$$P = \eta_v \rho^{\gamma_v} \quad (2)$$

$$E = \frac{\eta_v}{\gamma_v - 1} \rho^{\gamma_v - 1} \quad (3)$$

$$a_v^2 = \gamma_v \eta_v \rho^{\gamma_v - 1} \quad (4)$$

$$T = \frac{\eta_v}{R} \rho^{\gamma_v - 1} \quad (5)$$

where

$$\eta_v = \exp\left(\frac{S_0(\gamma_v - 1)}{R}\right) \quad (6)$$

$R$  is the universal gas constant,  $S_0$  is a constant entropy value, and  $a_v$  is the speed of sound in vapor. The liquid branch is described by the corresponding reduction of the stiffened polytropic EOS model [12]

$$P = (\gamma_l - 1)\rho(E + E_\infty) - \gamma_l P_\infty \quad (7)$$

where  $\gamma_l$  is the adiabatic exponent for the liquid, and  $P_\infty$  and  $E_\infty$  are two model parameters defining the maximum tension (the maximum value of the "negative pressure" achievable in the liquid) and the energy shift constant, correspondingly.  $E_\infty$  can be used to obtain the quantitative agreement of the internal energy of the liquid at normal conditions with experimental data. The reduced equations are

$$P = \eta_l \rho^{\gamma_l} - P_\infty \quad (8)$$

$$E = \frac{\eta_l}{\gamma_l - 1} \rho^{\gamma_l - 1} + \frac{P_\infty}{\rho} - E_\infty \quad (9)$$

$$a_l^2 = \gamma_l \eta_l \rho^{\gamma_l - 1} \quad (10)$$

$$T = \frac{\eta_l}{R_l} \rho^{\gamma_l - 1} \quad (11)$$

where

$$\eta_l = \exp\left(\frac{S_0(\gamma_l - 1)}{R_l}\right) \quad (12)$$

and  $a_l$  is the speed of sound in the liquid. The two branches are connected by a model for the liquid-vapor mixture

$$P = P_{\text{sat},l} + P_{vl} \log \left[ \frac{\rho_{\text{sat},v} a_{\text{sat},v}^2 [\rho_{\text{sat},l} + \beta (\rho_{\text{sat},v} - \rho_{\text{sat},l})]}{\rho_{\text{sat},l} [\rho_{\text{sat},v} a_{\text{sat},v}^2 - \beta (\rho_{\text{sat},v} a_{\text{sat},v}^2 - \rho_{\text{sat},l} a_{\text{sat},l}^2)]} \right] \quad (13)$$

where  $\rho_{\text{sat},v}$ ,  $\rho_{\text{sat},l}$ ,  $a_{\text{sat},v}$ ,  $a_{\text{sat},l}$  are the density and the speed of sound of vapor and liquid in saturation points, respectively,  $P_{\text{sat},l}$  is the liquid pressure in the saturation point,  $\beta$  is the void fraction

$$\beta = \frac{\rho - \rho_{\text{sat},l}}{\rho_{\text{sat},v} - \rho_{\text{sat},l}} \quad (14)$$

and the parameter  $P_{vl}$  is

$$P_{vl} = \frac{\rho_{\text{sat},v} a_{\text{sat},v}^2 \rho_{\text{sat},l} a_{\text{sat},l}^2 (\rho_{\text{sat},v} - \rho_{\text{sat},l})}{\rho_{\text{sat},v}^2 a_{\text{sat},v}^2 - \rho_{\text{sat},l}^2 a_{\text{sat},l}^2} \quad (15)$$

The expression (13) was derived by integrating an experimentally validated model for the sound speed in bubbly mixture [13,14]. A set of the EOS input parameters, most of which are measurable quantities, allows one to fit the two-phase EOS to thermodynamics data for real fluids. The selection of input parameters and some other details on the EOS model are presented in [6].

The most important feature of the homogenized isentropic EOS model is the correct behavior of the

sound speed in liquid at void fractions ranging from the pure liquid to pure vapor (gas) phases. Figure 1 depicts the dependence of pressure and sound speed on the averaged density of bubbly mercury obtained with this homogenized EOS model. This dependence agrees with experimental data and reflects the well-known fact [3] that the sound speed in bubbly liquid is lower than the sound speed in not only pure liquid but also in the pure vapor phase.

The homogenized equation of state has been validated through comparison to experimental data. In [6], the homogenized two-phase EOS model has been applied to study the interaction of mercury with an intensive proton pulse in the geometry typical for Neutrino Factory mercury target experiments. Obtained numerical results agree with experiments performed on the Alternating Gradient Synchrotron at the Brookhaven National Laboratory and On-Line Isotope Mass Separator facility (ISOLDE) at CERN [14,15]. The use of two-phase EOS has led to improvement over single-phase EOS simulations [16,17] of the mercury target experiments.

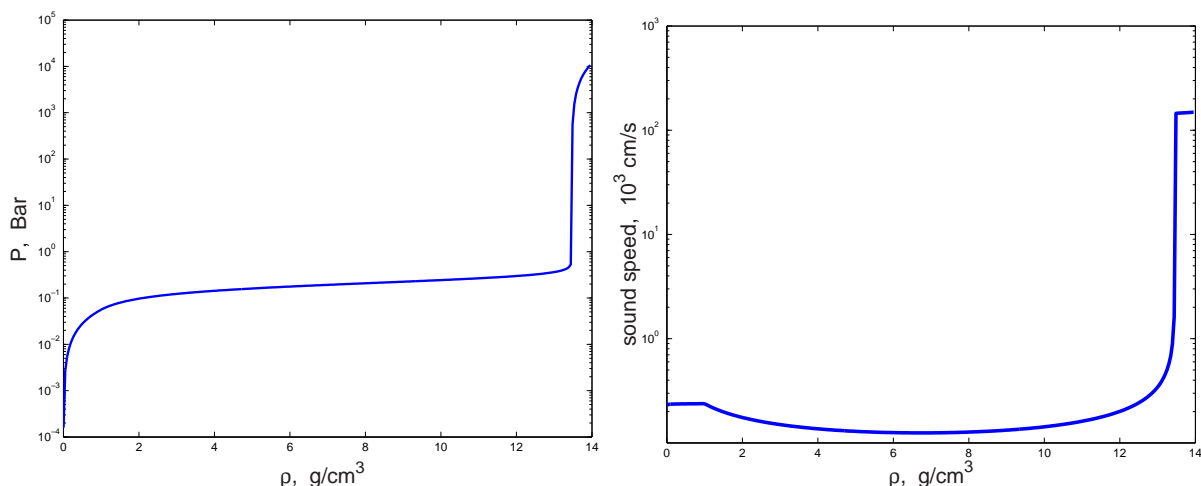


**FIGURE 1.** Pressure (left) and sound speed (right) as functions of density for bubbly mercury obtained using the homogenized EOS model

## 2.2 Heterogeneous Method

One of the main disadvantages of the homogenized equation-of-state model for multiphase flows is its inability to resolve spatial scales comparable to the distance between bubbles. In many cases, cavitation in strong rarefaction waves may lead to a rapid growth of a relatively small number of cavitation bubbles. Averaging of fluid properties will result in an unresolved fine structure of waves that may be critical for understanding the important features of the flow dynamics such as surface instabilities, bubble collapse induced pressure peaks, etc. The heterogeneous model eliminates this deficiency and improves many other thermodynamic and hydrodynamic aspects of the modeling of cavitating and bubbly flows.

In the heterogeneous method, we model a liquid-vapor or liquid-nondissolvable gas mixture as a system of one phase domains (vapor bubbles in a liquid) separated by free interfaces [8]. FronTier, a compressible hydrodynamics code with free interface support, is used to model the behavior of bubble interfaces. FronTier represents interfaces as lower dimensional meshes moving through a volume filling grid [5,11]. The traditional volume filling finite difference grid supports smooth solutions located in the region between interfaces. The dynamics of the interface comes from the mathematical theory of Riemann solutions, which are idealized solutions of single jump discontinuities for a conservation law. The FronTier code is capable of simultaneously tracking a large number of interfaces and resolving their topological changes (the breakup and merger of droplets) in two- and three-dimensional spaces. Away from interfaces, FronTier uses high-resolution hyperbolic techniques. Different equation-of-state models are used for gas and/or vapor bubbles and the ambient liquid. The method makes it possible to resolve spatial scales smaller than the typical distance between bubbles and to model some nonequilibrium thermodynamics features, such as finite critical tension in cavitating liquids.

Though computationally intensive, the heterogeneous model is potentially a very accurate technique, limited by only numerical errors. It allows one to account for drag, surface tension, and viscous forces as well as the phase transition induced mass transfer. We have recently developed a Riemann

solver governing the propagation of the liquid-vapor phase boundary. However, in the present simulations of mercury jets interacting with high-energy proton pulses, we neglect the phase transition induced mass transfer. Since characteristic time scales of hydrodynamics processes in such a jet are small, we assume that the evolution of cavitation bubbles is mainly due to the expansion (contraction) of the bubble content (mix of vapor and gas).

Numerical simulation of the cavitation presents additional complications, uncertainties, and numerical challenges compared to the simulation of wave phenomena in bubbly fluids (fluids containing small nondissolvable gas bubbles). These problems are associated with the dynamic creation and collapse of bubbles in the computational domain. The corresponding software routines were implemented in the FronTier code. A few remarks on modeling issues are necessary. According to the equilibrium thermodynamics approximation, liquid will vaporise when the pressure falls below the corresponding vapor pressure at given temperature. Liquids are able to sustain some amount of tension, which depends on their purity. The critical radius of the cavitation bubble is

$$R_c = \frac{2\sigma}{\Delta P_c} \quad (16)$$

where  $\sigma$  is the surface tension coefficient and  $\Delta P_c$  is the critical strength of the tensile pressure in the liquid. Initial cavitation bubble sizes in real liquids (for instance,  $R_c = 1 \mu\text{m}$  for mercury at  $P_c = 10$  bar) are close to numerically resolved limits as the FronTier code is equipped with the adaptive mesh refinement. However, we frequently use larger initial bubble size, especially for coarser grid computations in large domains. This is effectively equivalent to the insertion of a cavitation bubble at a later time. Since the evolution of liquid and vapor states during this short period of time is missing, initial states in the vicinity of the cavitation bubble contains some errors. We estimate, that these errors do not make a significant impact on the global dynamics.

To create such a nucleus with critical radius  $R_C$ , a critical energy  $E_C = 16\pi\sigma^3/3\Delta P_C^2$  [19] must be deposited into the liquid to break the barrier against nucleation. This critical energy  $E_C$  accounts only for surface energy and the gain in volume energy. The energy needed to convert liquid to vapor (heat

of vaporization) is neglected because it is relatively small. Within the homogeneous nucleation theory [19], one can write the nucleation rate  $J$

$$J = J_0 \exp^{E_C/(k_b T)} \quad (17)$$

per unit volume and per unit time. Here  $k_b$  is the Boltzmann's constant,  $T$  is the liquid temperature, and  $J_0$  is a factor of proportionality defined as

$$J_0 = N \left( \frac{2\sigma}{\pi m} \right)^{1/2} \quad (18)$$

where  $N$  is the number density of the liquid (molecules/m<sup>3</sup>) and  $m$  is the mass of a molecule. Thus, the nucleation probability  $\Sigma$  in a volume  $V$  during a time period  $t$  is [20]

$$\Sigma = 1 - \exp^{-J_0 V t \exp^{(-E_C/(k_b T))}} \quad (19)$$

Equations (16)–(19) allow one to relate a typical volume  $V$ , in which a nucleation bubble appears with probability  $\Sigma$  during time  $t$ , with the critical pressure. For  $\Sigma = 0.5$ , the critical pressure is

$$P_C \cong - \left( \frac{16\pi\sigma^3}{3k_b T \ln(J_0 V t / \ln 2)} \right)^{1/2} \quad (20)$$

The numerical time step defines a natural time scale  $t$  in Eq. (20), and  $V^{1/3}$  defines the spacing between

cavitation bubbles. Expressions (16)–(20), however, agree with experiments only in a relatively narrow thermodynamic region [19]. Therefore, there is some uncertainty in calculating the cavitation rate in numerical simulations if experimental data of the cavitation threshold and concentration of cavitation centers is unavailable for specific experimental conditions, especially if experiments deal with liquids with large amount of impurities due to interactions with intense beams of high energy particles typical for the Neutrino Factory/Muon Collider target.

### 2.3 Validation of Heterogeneous Numerical Model

In this section, we validate the heterogeneous numerical model through the study of the dynamics of linear and nonlinear waves in bubbly liquids. The schematic of the numerical experiment setup is depicted in Fig. 2. The liquid contains nondissolvable gas bubbles at normal conditions. The region around a long column of bubbles was chosen as the computational domain. As the first-order approximation, we can assume that the pressure waves are axisymmetric. The influence of neighboring bubbles can be effectively approximated by the Neumann boundary condition on the domain walls. Therefore, the wave propagation in bubbly flows was reduced to an axisymmetric two-dimensional problem.

Our first numerical experiments were performed with small amplitude linear waves in bubbly flu-

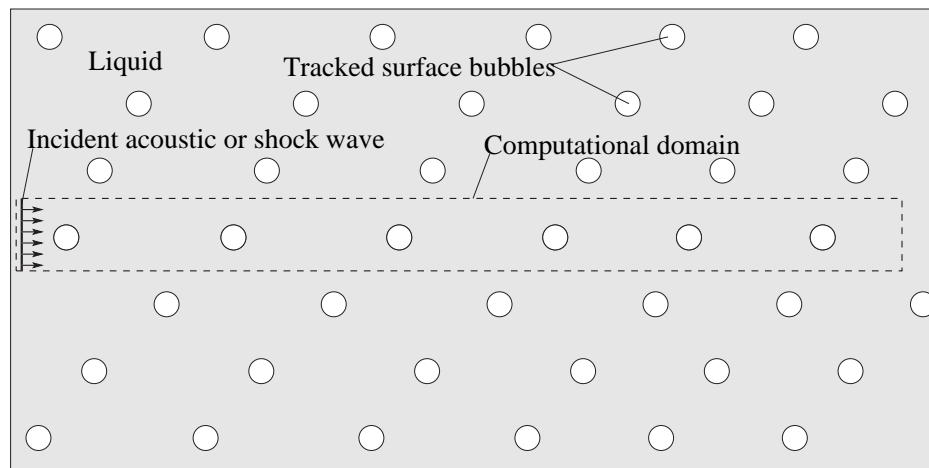


FIGURE 2. Schematic of the numerical experiment. The computational domain contained 100 bubbles

ids. The theoretical dispersion relation for linear sound waves in bubbly fluids can be derived from the wave equations [4]. The dispersion relation is

$$\frac{k^2}{\omega^2} = \frac{1}{c_f^2} + \frac{1}{c^2} \frac{1}{1 - i\delta \frac{\omega}{\omega_B} - \frac{\omega^2}{\omega_B^2}} \quad (21)$$

where  $\omega_B$  is the resonant frequency of single bubble oscillation,  $\delta$  is the damping coefficient accounting for the various dissipation mechanisms.  $c_f$  is the sound speed in bubble free fluid and  $c$  is the sound speed in the low-frequency limit, which is given by

$$\frac{1}{c^2} = [\beta \rho_g + (1 - \beta) \rho_f] \left( \frac{\beta}{\rho_g c_g^2} + \frac{1 - \beta}{\rho_f c_f^2} \right)$$

where  $\rho_g$  and  $\rho_f$  are densities of the gas and the fluid,  $c_g$  and  $c_f$  are sound speeds of the two phases, while  $\beta$  is the volume fraction of the bubbles. Measuring the dispersion relation and the attenuation rates from simulations, we found that results are in good agreement with theoretical predictions. The numerical and theoretical results are depicted in Fig. 3.

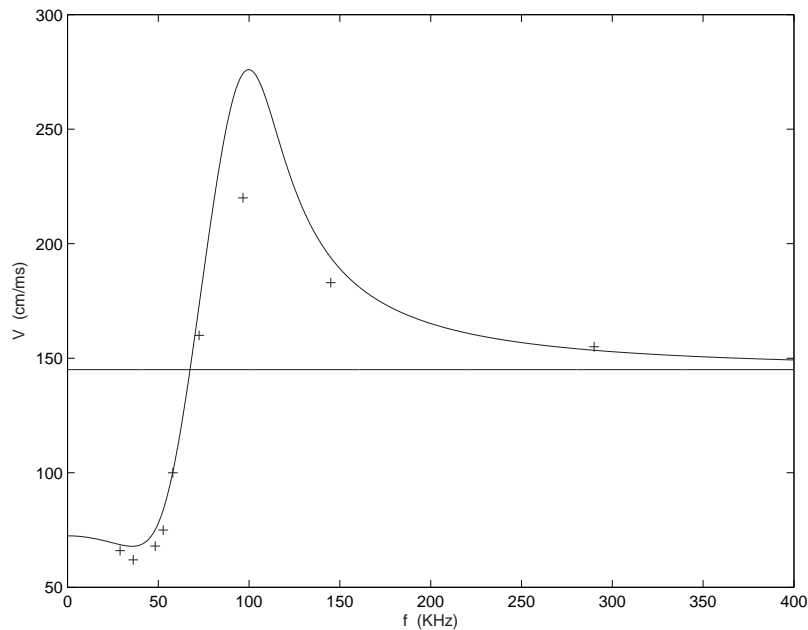
As another numerical experiment, we measured shock velocities and plotted shock profiles for bubbles consisting of different kinds of gases. The shock speeds agreed with the theoretical prediction of [3] very well (with the difference of  $< 3\%$ ). The shock profiles were measured at 1.0 m away from the shock incident plane as in the experiments of Beylich and Gülhan [1]. The shock profiles in glycerol filled with SF<sub>6</sub> bubbles of volume fraction 0.25% are plotted in Fig. 4. Some discrepancy in the amplitude and the period of pressure oscillations can be explained by grid related numerical errors. Current simulations performed on  $90 \times 10800$  grids required several days of CPU time on a parallel cluster of Pentium processors. To improve the accuracy and performance of the heterogeneous model, we have been working on the adaptive mesh refinement method for the FronTier code. Both simulations and experiments showed that the amplitude of pressure oscillations in the bubbly layer after the passage of the shock front is smaller for the gas with larger polytropic index.

### 3. COMPARISON OF HETEROGENEOUS AND HOMOGENIZED MODELS

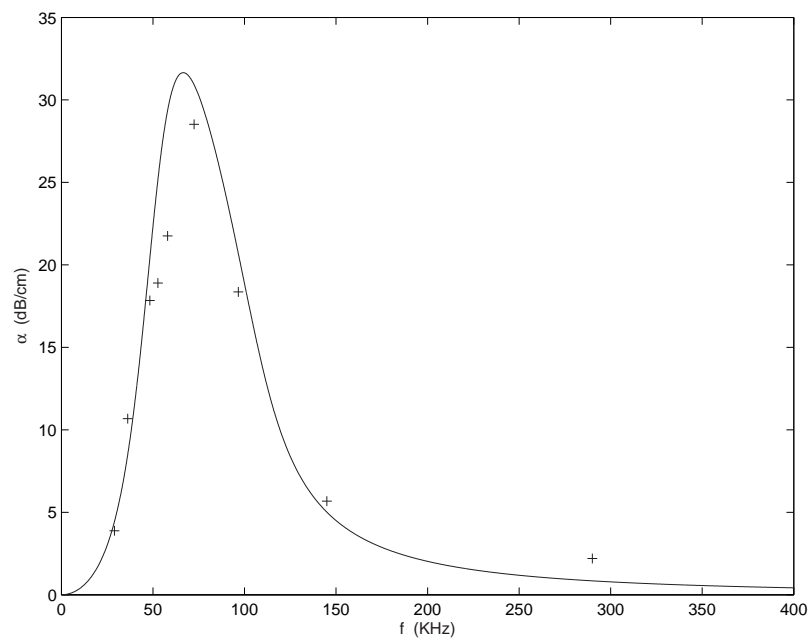
In this section, we apply two approaches for modeling cavitating and bubbly flows to the study of a free mercury jet interacting with high-energy proton pulses. Such a jet is a key component of the target for the proposed Neutrino Factory/Muon Collider [21,10]. The target is shown schematically in Fig. 5. It will contain a series of mercury jet pulses of about 0.5 cm in radius and 60 cm in length. Each pulse will be shot at a velocity of 30–35 m/s into a 20 Tesla magnetic field at a small angle (0.1 rad) to the axis of the field. When the jet reaches the center of the magnet, it will interact with a 3 ns proton pulse depositing about 100 J/g of energy in the mercury.

In numerical simulations, the initial mercury jet was taken as a 15 cm long and 1 cm diameter cylinder with small initial surface perturbations. 2D axisymmetric geometry was used. In the present studies of cavitation processes, the effect of the magnetic field was not considered. The MHD processes in one-phase liquid mercury jet were studied in [16,17]. Combining of MHD with cavitation models is in progress, and results will be presented in a forthcoming paper. The influence of the proton pulse was modeled by adding the proton beam energy density to the internal energy density of mercury at a single time step. For all simulations presented in this paper, the proton energy deposition in mercury was approximated by a 2D Gaussian distribution that accurately reproduces the actual beam energy deposition achieved in corresponding experiments.

The external energy deposition in the mercury jet resulted in the instantaneous heating and formation of a high-pressure domain and strong waves. After the initial compression wave, the rarefaction wave in the mercury jet significantly exceeded the mercury cavitation threshold, which was approximately estimated in [22] as  $P_c = -10$  bar. Our previous simulations of the mercury jet interaction with a proton pulse using one phase liquid equation of state for mercury [16,17] neglected cavitation and its influence on the wave and interface dynamics. As a result, simulations were able to reproduce only qualitatively the state of the target after the interaction, namely, the jet breakup and dispersion into small radial jets and droplets. The result of this jet breakup was however caused by multiple jet oscil-



(a)



(b)

**FIGURE 3.** Comparison of the dispersion relation between the simulation and the theory.  $R = 0.06$  mm,  $\beta = 0.02\%$ , the equilibrium pressure is 1.0 bar, and the amplitude of the incident pressure wave is 0.1 bar. Grid resolution is 100 grid/mm. (a) is the phase velocity, (b) is the attenuation coefficient. In both (a) and (b), the crosses are the simulation data and the solid line is the theoretical prediction from Eq. (21) with  $\delta = 0.7$ . The horizontal line in figure (a) is the sound speed in pure water

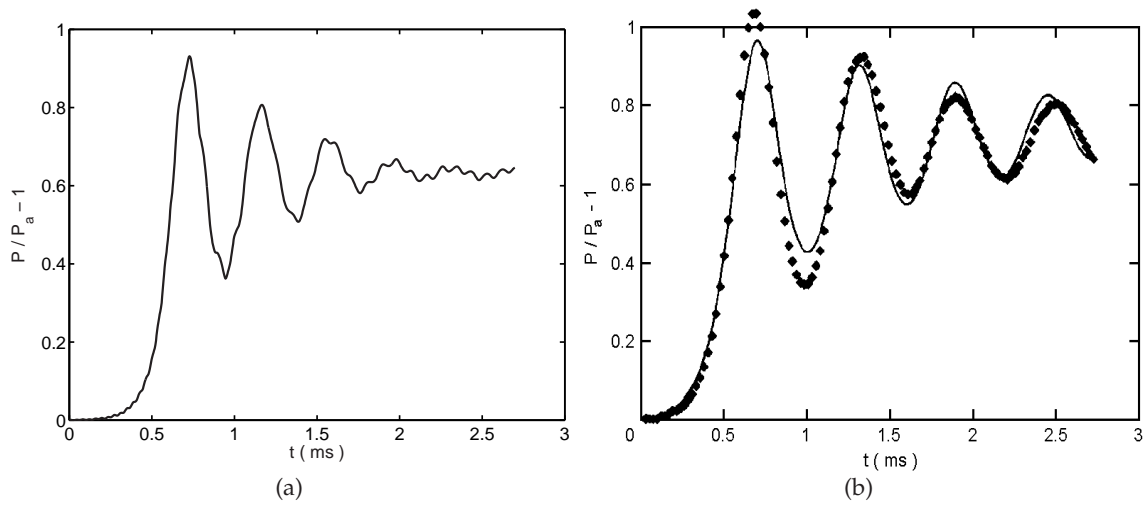


**FIGURE 4.** Shock profiles in glycerol filled with  $\text{SF}_6$  ( $\gamma = 1.09$ ) bubbles. The parameters in the simulations are from the experiments of Beylich and Gülhan [1]. Initial bubble radius is 1.15 mm, and  $\beta = 0.25\%$ . Initial pressure is 1.11 bar, and the pressure behind the shock is 1.80 bar. (a) is from the simulation, (b) is from the experiment. The solid curve in (b) is the author's original fitting with artificial turbulent viscosity

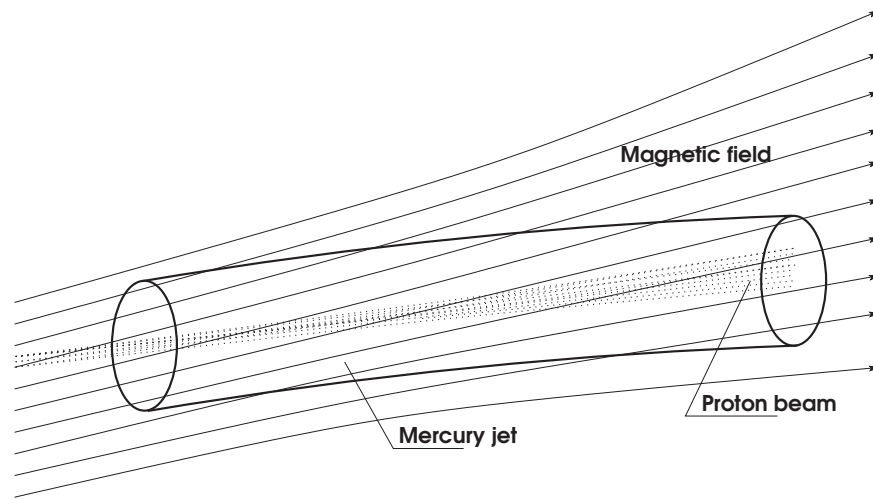


**FIGURE 5.** Schematic of the Neutrino Factory/Muon Collider target

lations due to the liquid tension and a cascade of interactions of the free surface with reflected waves. Such jet oscillations have not been observed experimentally. Taking into account the strength of rarefaction waves observed in numerical simulations with a single fluid EOS, it is clear that cavitation of mercury must occur at such conditions, and the corresponding mitigation of rarefaction waves by expanding cavitation bubbles. Accounting for cavita-

tion in the mercury jet completely changed the dynamics of waves and the mercury-free surface.

Our first set of numerical simulations of cavitation in the mercury jet was based on the homogenized two phase EOS model. The model parameters, such as the density, pressure, sound speed, and temperature of both liquid- and vapor-saturated points, were chosen based on the ANEOS thermodynamic mercury database of Sandia National Lab-

oratory. Numerical results showed the formation of a large liquid-vapor mixture domain along the jet axes. The average velocity of the jet surface was much smaller compared to one-phase liquid simulations and agreed with experimentally measured values [14,15].

The second set of numerical experiments employed the direct simulation of cavitation bubbles. The dynamic interface insertion algorithm was used to create bubbles in rarefaction waves with tension exceeding the of critical value of 10 bar. Since the distribution of cavitation centers could not be calculated exactly, different concentrations of bubbles were used in numerical simulations. Figure 6 depicts the density distribution in the mercury jet showing vapor cavities at 50 ms after the interaction with the proton pulse depositing 100 J/g of energy in the jet center.

The evolution of the two phase domain in the mercury jet observed using the heterogeneous model was very similar to one obtained with the homogenized model and not very sensitive to changes in the concentration of nucleation centers or the critical pressure  $P_c$ . Namely, we did not observe essential changes of the average velocity of the mercury jet surface at different values of  $P_c$ . A possible explanation is that the rapid pressure relaxation in bubbly fluids weakens strong waves. In this case, the expansion of the two-phase domain is driven by inertial forces due to the radial momentum gained during short period of time after the interaction with the proton pulse. Figure 7 depicts the distribution of densities in the cross section of the mercury jet obtained with the homogenized and heterogeneous models, and the experimental image of the jet. The time dependence of the maximal jet radius predicted by both cavitation models is shown in Fig. 8(a). The average jet surface velocity dur-

ing 160 ms time interval predicted by two models is within 14%. Two models also predict a similar increase of the jet expansion velocity with the increase of the proton beam intensity. Figure 8(b) shows maximal jet surface velocities at various values of the peak energy deposition. Therefore, two models with such different physics assumptions and numerical techniques agree reasonably well in predicting the formation and evolution of the two-phase cavitation region and the jet expansion. The calculated jet velocities were in the range of experimentally measured values [5]. More close comparison of the calculated jet evolution with experiments is not possible due to limited experiemntal data.

We believe that one of the most essential differences between the homogenized and heterogeneous models is associated with the range of numerically resolved spatial scales. Because of the averaging of fluid properties on the large length scale compared to the distance between bubbles, the homogenized model is not capable of resolving fine structure of waves in the fluid volume and small-scale surface perturbations. The heterogeneous model is free of this deficiency. Using the later technique, we were able to obtain disintegration of the jet (see Fig. 9). This breakup was observed at low concentration of cavitation bubbles. In the future work, we will investigate the role of other factors that may improve the simulation of the jet breakup, such as collapses of small bubbles due to surface tension and corresponding pressure peaks and flow perturbations.

Based on our experience with flow regimes, which are beyond the scope of this paper, two models perform differently in multiphase flows if the phase transition induced mass transfer is not negligible. The explicit tracking of phase boundaries and solving the phase transition equations produces accurate solutions, whereas the homogenized model

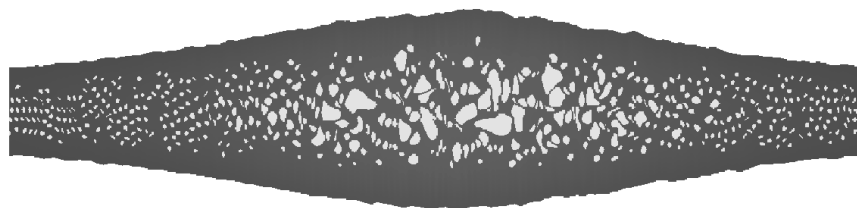


**FIGURE 6.** Cavities in the mercury jet at 50 microseconds after the interaction with the proton pulse

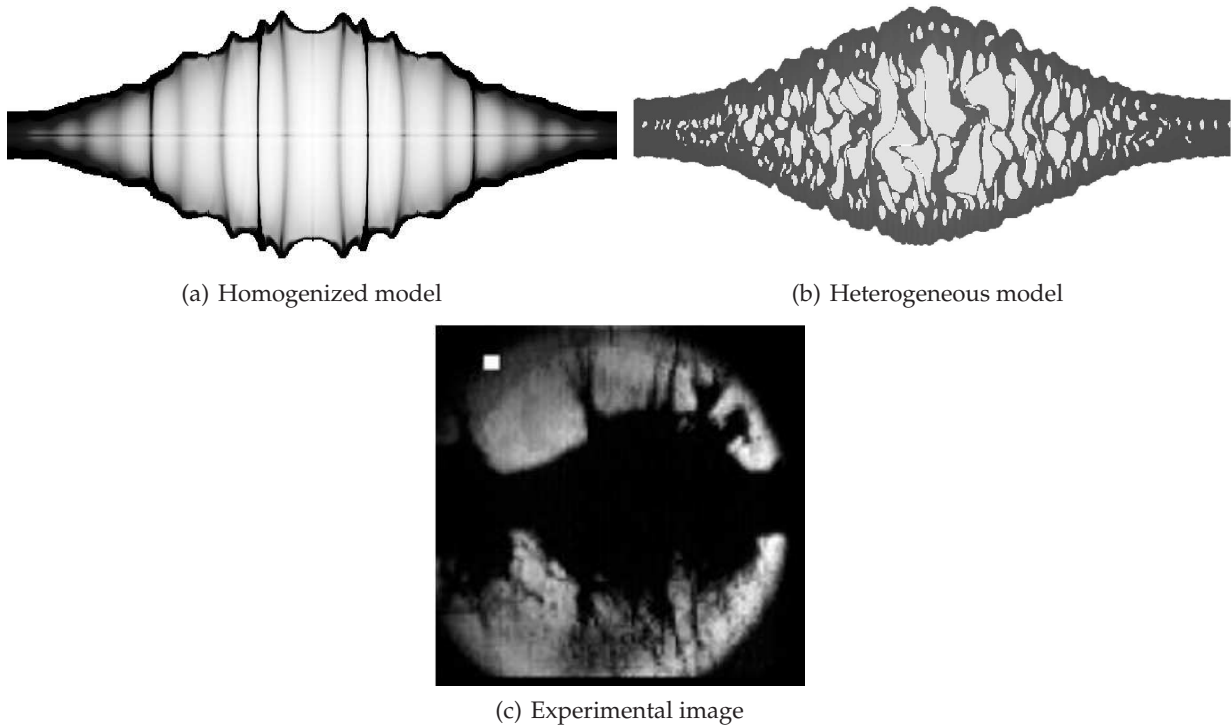


**FIGURE 7.** Comparison of the homogenized and heterogeneous numerical models, and experimental results. Density distribution in the mercury jet obtained using (a) the homogenized EOS model and (b) heterogeneous model. (c) Experimental image of the mercury jet

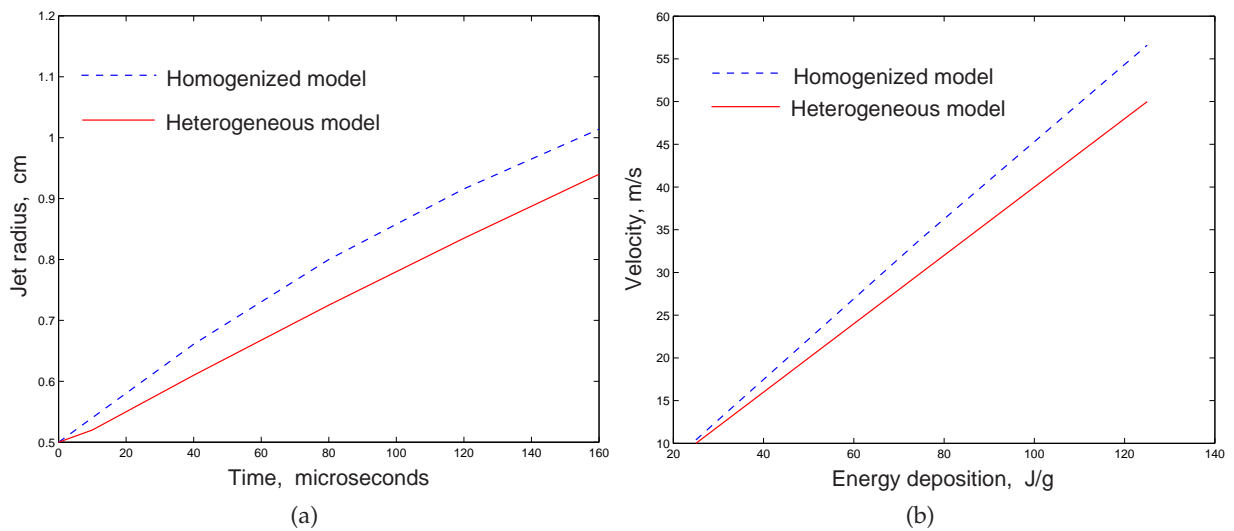


**FIGURE 8.** (a) Time dependence of the maximal jet radius predicted by the homogenized model (dashed line) and the heterogeneous model (solid line). (b) Dependence of the maximal jet surface velocity at 100 ms on the amount of deposited energy

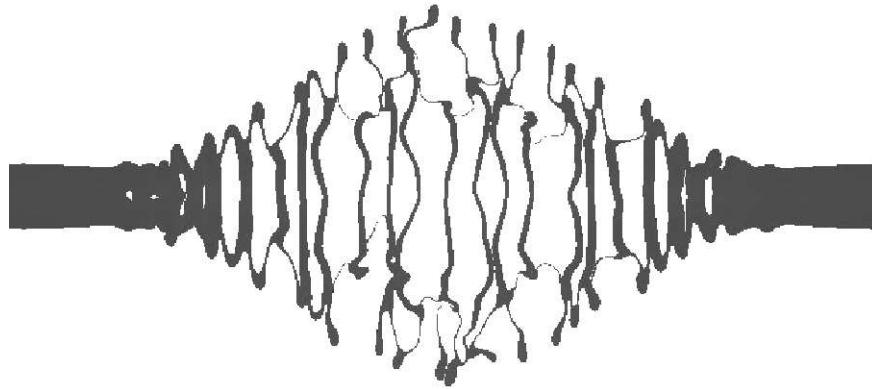


FIGURE 9. Disintegration of the jet caused by the evolution of cavities

does not have capabilities to resolve these complex physics processes. The difference between two cavitation models could also play an important role in the study of other processes in the mercury jet, such as magnetic-field-induced eddy currents and MHD forces, as the explicit tracking of cavitation bubbles changes the connectivity of mercury in the expanding jet.

#### 4. CONCLUSIONS

We have applied the heterogeneous and homogenized numerical models to the simulation of free surface multiphase flows of cavitating liquids. The heterogeneous model is based on the ability of our hydrodynamics code FronTier to explicitly track complex interfaces and resolve their topological changes. The method has numerous potential advantages and applications. It is capable of resolving small spatial scales and accounting for drag, surface tension, and viscous forces, and the phase transition induced mass transfer. It is, however, prohibitively computationally expensive for large 3D domains.

The second method uses a homogenized description of bubbly and/or cavitating fluids by averaging their properties on large length scales compared to the distance between bubbles. The method is based on the reduction to a single isentrope of well-known models describing pure liquid and vapor phases, and a consistent connection of them by a pressure model for the mixed phase. Despite being simple and computationally inexpensive, the method is sufficiently accurate within its domain of validity and applicable to a variety of practically important

problems. The method has been validated through the study of the interaction of mercury with intensive proton pulses in the geometry typical for Neutrino Factory liquid mercury target experiments. The simulations are in good quantitative agreement with experiments. Through the comparison of numerical simulations with experiments and theoretical predictions on the propagation of linear and shock waves in bubbly fluids, the heterogeneous approach has also been validated. The heterogeneous and homogenized approaches are complementary and can be used to resolve different temporal and spatial scales in numerical simulations.

Two methods have been compared through the study of cavitation in a free mercury jet interacting with high-energy proton pulses. Such a jet is a key component of the target for the proposed Neutrino Factory/Muon Collider. The two methods showed a good agreement of the mercury jet surface velocity and the evolution of the liquid-vapor mixture domain. The heterogeneous model, due to its ability to resolve fine structure of waves and small spatial scales, was superior in the simulation of long-time jet evolution, namely, the disintegration of the mercury jet. The heterogeneous method has the ability to accurately simulate the phase transition induced mass transfer and thus has advantages for phase transition dominated flows.

The deficiencies of the heterogeneous method are associated with the absence of experimental data and satisfactory modeling of the distribution of cavitation centers, and errors due to limited numerical resolution, especially at initial stages of the cavita-

tion bubble formation and late stages of the bubble collapse. Although the first issue can be resolved by additional experimental studies and the benchmark of models for the distribution of cavitation centers, the second problem can be improved by the adaptive mesh refinement. In the present simulation of the mercury jet cavitation, errors due to uncertainties in the critical pressure and distribution of cavitation centers did not affect the global behavior of the jet as both heterogeneous and homogeneous methods were in good quantitative agreement. However, we expect that more accurate resolution of these problems may become necessary for the simulation of processes which depend on the small-scale structure of the multiphase domain, such as magnetohydrodynamics.

## ACKNOWLEDGMENT

We thank members of the Neutrino Factory/Muon Collider Collaboration for useful discussions and for partial support of work presented here.

*This manuscript has been authored in part by Brookhaven Science Associates, LLC, under Contract No. DE-AC02-98CH10886 with the U.S. Department of Energy. The United States Government retains, and the publisher, by accepting the article for publication, acknowledges, a world-wide license to publish or reproduce the published form of this manuscript, or allow others to do so, for the United States Government purpose.*

## REFERENCES

1. Beylich, A. E., and Gülhan, A., On the structure of nonlinear waves in liquids with gas bubbles. *Phys. Fluids A*, **2**:1412–1428, 1990.
2. Cafilisch, R. E., Miksis, M. J., Papanicolaou, G. C., and Ting, L., Effective equations for wave propagation in bubbly liquids. *J. Fluid Mech.*, **153**:259–273, 1985.
3. Watanabe, M. and Prosperetti, A. Shock waves in dilute bubbly liquids. *J. Fluid Mech.*, **274**:349–381, 1994.
4. Wijngaarden, L. Van., One-dimensional flow of liquids containing small gas bubbles. *Ann. Rev. Fluid Mech.*, **4**:369–396, 1972.
5. Glimm, J., Grove J., Li, X.-L., and Tan, D. C., Robust computational algorithms for dynamic interface tracking in three dimensions. *SIAM J. Sci. Comp.*, **21**:2240–2256, 2000.
6. Samulyak, R., and Prykarpatsky, Y., Richtmyer-Meshkov instability in liquid metal flows: influence of cavitation and magnetic fields. *Math. Comput. Simul.*, **65**:431–446, 2004.
7. Matsumoto, Y., and Takemura, F., Influence of internal phenomena on gas bubble motion. *JSME Int. J.*, **37**:288–296, 1994.
8. Welch, S. W., Local simulation of two-phase flows including interface tracking with mass transfer. *J. Comp. Phys.*, **121**:142–154, 1995.
9. Juric, D., and Tryggvason, G., Computation of boiling flows. *Int. J. Multiphase Flow*, **24**:387–410, 1998.
10. Ozaki, S., Palmer, R., Zisman, M., and Gallardo, J., Eds. Feasibility Study– II of a Muon-Based Neutrino Source. BNL-52623, 2001.
11. Glimm, J., Grove, J. W., Li, X. L., Shyue, K. M., Zhang, Q., and Zeng, Y., Three dimensional front tracking. *SIAM J. Sci. Comp.*, **19**:703–727, 1998.
12. Menikoff, R., and Plohr, B., The Riemann problem for fluid flow of real materials. *Rev. Mod. Phys.*, **61**:75–130, 1989.
13. Wallis, G. B. *One-Dimensional Two-phase Flow.*, McGraw-Hill, New York, 1969.
14. Fabich, A., and Lettry J., Experimental observation of proton-induced shocks and magneto-fluid-dynamics in liquid metal. In *Proceedings NuFact 01*, Nuclear Instr. and Methods A, **503**:336–339, 2003.
15. Kirk, H., et al, Target studies with BNL E951 at the AGS. Particles and Accelerators 2001. June 18-22, 2001, Chicago.
16. Samulyak, R., Glimm, J., Oh, W., Kirk, H., and McDonald, K., Numerical simulation of free surface MHD flows: Richtmyer-Meshkov instability and applications. *Lect. Notes Comp. Sci.*, **2667**:558–567, 2003.
17. Samulyak, R., Numerical simulation of hydro- and magnetohydrodynamic processes in the Muon Collider target. *Lect. Notes Comp. Sci.*, **2331**:391–400, 2002.

18. Samulyak, R., Lu, T., and Prykarpatskyy, Y., Direct and homogeneous numerical approaches to multiphase flows. *Lect. Notes Comp. Sci.*, **3039**:653–660, 2004.
19. Brennen, C. E., *Cavitation and Bubble Dynamics*. Oxford University Press, London, 1995.
20. Balibar, S., and Caupin, F., Metastable liquids. *J. Phys: Condensed Matter*, **15**:s75–s82, 2003.
21. Alsharoá, M. et al., Recent progress in neutrino factory and muon collider research within the Muon Collaboration. *Phys. Rev. Special Topics*, **6**(8):081001-1–081001-52, 2003.
22. West, C. D., Cavitation in a mercury target. ORNL/TM-2000/263, 2000.